

---

---

# An Imaging Comparison of $^{64}\text{Cu}$ -ATSM and $^{60}\text{Cu}$ -ATSM in Cancer of the Uterine Cervix

Jason S. Lewis<sup>1,2</sup>, Richard Laforest<sup>1,2</sup>, Farrokh Dehdashti<sup>2,3</sup>, Perry W. Grigsby<sup>2,4</sup>, Michael J. Welch<sup>1,2</sup>, and Barry A. Siegel<sup>2,3</sup>

<sup>1</sup>Division of Radiological Sciences, Mallinckrodt Institute of Radiology, St. Louis, Missouri; <sup>2</sup>Alvin J. Siteman Cancer Center, Washington University School of Medicine, St. Louis, Missouri; <sup>3</sup>Division of Nuclear Medicine, Mallinckrodt Institute of Radiology, St. Louis, Missouri; and <sup>4</sup>Department of Radiation Oncology, Washington University School of Medicine, St. Louis, Missouri

---

Tumor uptake of copper(II)-diacetyl-bis(*N*<sup>4</sup>-methylthiosemicarbazone) (copper-ATSM), a hypoxia-targeting radiopharmaceutical, assessed by PET has been found to correlate with prognosis in several human cancers. Wide clinical utility of this tracer will require its labeling with a copper radionuclide having a longer half-life than the  $^{60}\text{Cu}$  used in studies to date. The purpose of this work was to obtain the requisite preclinical data for copper-ATSM to file an investigational new drug application, followed by a crossover comparison of PET image quality and tumor uptake with  $^{60}\text{Cu}$ -ATSM and  $^{64}\text{Cu}$ -ATSM in women with cancer of the uterine cervix. **Methods:** The preclinical toxicology and pharmacology of a copper-ATSM formulation was examined using standard *in vitro* and *in vivo* assays, as well as 14-d toxicity studies in both rats and rabbits. For the clinical test-retest imaging study, 10 patients with cervical carcinoma underwent PET on separate days with  $^{60}\text{Cu}$ -ATSM and  $^{64}\text{Cu}$ -ATSM. Image quality was assessed qualitatively, and the tumor-to-muscle activity ratio was measured for each tracer. **Results:** The toxicology and pharmacology data demonstrated that the formulation has an appropriate margin of safety for clinical use. In the patient study, we found that the image quality with  $^{64}\text{Cu}$ -ATSM was better than that with  $^{60}\text{Cu}$ -ATSM because of lower noise. In addition, we found that the pattern and magnitude of tumor uptake of  $^{60}\text{Cu}$ -ATSM and  $^{64}\text{Cu}$ -ATSM on studies separated by 1–9 d were similar. **Conclusion:**  $^{64}\text{Cu}$ -ATSM appears to be a safe radiopharmaceutical that can be used to obtain high-quality images of tumor hypoxia in human cancers.

**Key Words:** Cu-ATSM; hypoxia;  $^{60}\text{Cu}$ ;  $^{64}\text{Cu}$ ; cervical cancer

**J Nucl Med 2008; 49:1177–1182**  
DOI: 10.2967/jnumed.108.051326

---

**T**umor uptake of copper(II)-diacetyl-bis(*N*<sup>4</sup>-methylthiosemicarbazone) (copper-ATSM) (1,2), a hypoxia-targeting radiopharmaceutical, as assessed by PET, has been confirmed as a clinically important biomarker of prognosis in

several human cancers. Copper-ATSM PET has been shown to distinguish patients likely and unlikely to respond to conventional therapies for cancers of the lung (3), uterine cervix (4,5), rectum (6), and head and neck (Chao, unpublished data, 2002).

Most clinical copper-ATSM studies have used the agent labeled with the short-lived positron-emitting radionuclide of copper (7),  $^{60}\text{Cu}$  (half-life, 0.395 h;  $\beta^+$ -decay, 92.5%; electron capture, 7.5%) (3–6,8). To enable copper-ATSM to be translated for use in PET centers that do not have an in-house cyclotron, copper-ATSM labeled with one of the longer-lived positron-emitting nuclides,  $^{64}\text{Cu}$  (half-life, 12.7 h;  $\beta^+$ -decay, 17.4%;  $\beta^-$ -decay, 38.5%; electron capture, 43%) or  $^{61}\text{Cu}$  (half-life, 3.33 h;  $\beta^+$ -decay, 62%; electron capture, 38%) (7), is required. The longer half-lives of  $^{64}\text{Cu}$  and  $^{61}\text{Cu}$  allow for production at a regional center and distribution to PET facilities in a fashion similar to that for  $^{18}\text{F}$ -labeled radiopharmaceuticals. The preparation of  $^{62}\text{Cu}$  (half-life, 0.16 h;  $\beta^+$ -decay, 98%; electron capture, 2%), via a  $^{62}\text{Zn}/^{62}\text{Cu}$  generator system, has been reported and commercialized (9) and offers an additional method for radiolabeling copper-ATSM for use in humans.

The initial clinical studies of  $^{60}\text{Cu}$ -ATSM (3–6,8) in cancers were undertaken at Washington University School of Medicine under the auspices of the Radioactive Drug Research Committee and in accordance with 21 Code of Federal Regulations 361.1 to obtain basic information on the metabolism (including kinetics, distribution, dosimetry, and localization) of copper-ATSM. These preliminary observations encouraged us to pursue confirmation of our findings in a larger, multicenter clinical trial. For such a trial to be undertaken within the United States, it was necessary to apply to the U.S. Food and Drug Administration (FDA) for investigational use of  $^{64}\text{Cu}$ -ATSM, thus allowing for production and shipping of the longer-lived radiopharmaceutical to imaging centers. This article describes the first clinical study undertaken after filing of the investigational new drug (IND) application that compares the image quality of  $^{60}\text{Cu}$ -ATSM and  $^{64}\text{Cu}$ -ATSM (test-retest) in a cohort of 10 women with cervical carcinoma.

---

Received Feb. 1, 2008; revision accepted Apr. 7, 2008.  
For correspondence or reprints contact: Jason S. Lewis, Department of Radiology, Memorial Sloan-Kettering Cancer Center, 1275 York Ave., New York, NY 10065.  
E-mail: lewisj2@mskcc.org  
COPYRIGHT © 2008 by the Society of Nuclear Medicine, Inc.

## MATERIALS AND METHODS

### General

All chemicals, unless otherwise stated, were purchased from Sigma-Aldrich Chemical Co., Inc. All solutions were prepared using distilled, deionized water (>18 M $\Omega$  resistivity) by passing through a Milli-Q filtration system (Millipore Corp.).

### Toxicology Formulation (Copper-ATSM/H<sub>2</sub>ATSM)

Guidance from the FDA was obtained in pre-IND discussions regarding the formulation of the agent to be tested. The selected formulation represented a worst-case scenario, based on the final composition of <sup>64</sup>Cu-ATSM at the time of injection into humans. The formulation consisted of the following components: 2.1556 g of H<sub>2</sub>ATSM (69.73%), 153.9 mg of nonradioactive copper-ATSM (4.98%), 12.0 mg of CoCl<sub>2</sub> (0.38%), and 0.77 g of NiCl<sub>2</sub> (24.91%). These 4 solid materials were ground and mixed to produce a homogeneous mixture. The solid formulation was then dissolved in dimethylsulfoxide (1%), ethanol (5%), and saline (94%) before use in the preclinical toxicology studies.

### Toxicology and Pharmacology Studies

The preclinical toxicology and pharmacology of a copper-ATSM formulation was examined using standard *in vitro* and *in vivo* assays, as well as 14-d toxicity studies in both rats and rabbits. All toxicology and pharmacology studies were conducted in compliance with good laboratory practice regulations (21 Code of Federal Regulations, part 58). Mutagenicity was determined with the *in vitro* *Salmonella* reverse-mutation plate-incorporation assay, the *in vitro* L5178Y/TK<sup>+/-</sup> mouse lymphoma mutation assay, and the *in vivo* micronucleus assay in rats. Safety pharmacology studies were performed by cardiovascular and pulmonary safety testing on beagle dogs and neurologic safety assessment on rats. A 14-d toxicity study of the toxicology formulation in rats and rabbits was also performed. The full experimental details, protocols, and results of these evaluations can be accessed at <http://imaging.cancer.gov/programsandresources/specializedinitiatives/dcide/page13>.

### Radiopharmaceutical Synthesis

<sup>60</sup>Cu and <sup>64</sup>Cu were produced in the CS15 cyclotron (Cyclotron Corp.) at the Washington University Medical Center, as previously described (10,11). <sup>60</sup>Cu-ATSM and <sup>64</sup>Cu-ATSM were produced on the basis of methods previously described (3,5). The methods for production are identical for both compounds. The final sterile, apyrogenic, and isotonic <sup>60</sup>Cu-ATSM or <sup>64</sup>Cu-ATSM solution had greater than 98% radiochemical purity at the time of injection.

### PET Phantom Analysis

The PET image-quality accreditation phantom (12) of the American College of Radiology was used to compare the quantitative accuracy of <sup>64</sup>Cu and <sup>60</sup>Cu imaging in the ECAT HR+ scanner (Siemens-CTI). The performance specifications of this scanner have been previously reported (13). The scanner has a spatial resolution of 4.5 mm in full width at half maximum for imaging with short-range positron emitters such as <sup>18</sup>F or <sup>64</sup>Cu. The phantom is composed of a cylinder 20 cm in diameter and 20 cm long, with fillable cylinders attached to the top lid. The diameter of these cylinders is 8, 12, 16, and 25 mm, and their length is 25 mm. The phantom was prepared with a 9.87:1 activity ratio between the cylinders and the surrounding background area. The lower part of the phantom, which contains a pattern of cold rods of various diameters in a pielike configuration, was not analyzed in this work. Peak and average activity concentrations in the cylinders were compared with the

average activity in the uniform area to calculate ratios to mimic the tumor-to-muscle ratios from the patient data analysis. The <sup>64</sup>Cu experiment was done by preparing 13.0 MBq (0.352 mCi) of <sup>64</sup>Cu diluted in 600 mL. This solution was then used to fill the cylinders. The rest of the solution was placed in the uniform area of the phantom, and water was added to completely fill the phantom for a total volume of 5.92 L. For the <sup>60</sup>Cu experiment, the initial activity was 72.15 MBq (1.95 mCi). These values correspond to an injected patient activity of 185 MBq (5 mCi) and 925 MBq (25 mCi), respectively, assuming a typical patient weight of 70 kg. The phantoms were then scanned for 1 h, with the same acquisition protocol as for patients (2-dimensional [2D] for <sup>60</sup>Cu and 3-dimensional [3D] for <sup>64</sup>Cu), and the images were reconstructed using the same algorithm (ordered-subsets expectation maximization, 2D, 2 iterations/32 subsets, with a Hann filter at 0.3 cm<sup>-1</sup> followed by a 3D gaussian filter of 7.5 mm). Regions of interest were drawn on the hot cylinders at 50%, 50%, 40%, and 25% of the maximum inside the 25-, 16-, 12-, and 8-mm cylinders, respectively. The attenuation correction was measured by a 10-min transmission scan using the three <sup>68</sup>Ge rotating rod sources of the camera followed by the manufacturer's segmentation algorithm.

### Treatment of Cascade Coincidences in <sup>60</sup>Cu Imaging

Given that <sup>60</sup>Cu decays by positron decay with the concurrent emission of numerous cascade  $\gamma$ -photons, the fortuitous cascade coincidences were removed by convolution of the cascade  $\gamma$ -ray kernel as previously reported (14,15) and validated for <sup>86</sup>Y and <sup>76</sup>Br imaging in clinical cameras. Using this technique, the fully corrected projection data (corrected for normalization, attenuation, and scatter) were further corrected by subtraction of the cascade background, and the images were then reconstructed from those corrected data with the same reconstruction algorithm. All imaging with <sup>60</sup>Cu was performed in 2D mode because the collimator septa minimize contamination by cascade coincidences.

### Human PET

The comparison study was performed under the auspices of IND 62,675. To test the safety of <sup>60</sup>Cu-ATSM and <sup>64</sup>Cu-ATSM, we monitored the vital signs of the participants and the results of their various laboratory tests, including a standard complete blood cell count, a comprehensive metabolic panel, and urinalysis, within 4 h before and 1 h to 7 d after radiopharmaceutical injection. All examinations were monitored for clinically significant changes that may have been related to copper-ATSM administration. A change in heart rate of more than 20 beats/min or in systolic or diastolic blood pressure of more than 20 mm Hg was considered to be significant. A change in hemoglobin of more than 2 g/dL, in serum glutamate pyruvate transaminase of more than 150 IU/L, in total bilirubin of more than 0.5 mg/dL, or in serum creatinine of more than 0.75 mg/dL was also considered to be significant. This investigation was approved by the Human Research Protection Office and the Radioactive Drug Research Committee of Washington University School of Medicine and by the Protocol Review and Monitoring Committee of the Siteman Cancer Center. Ten women with newly diagnosed squamous cell carcinoma of the uterine cervix underwent PET with both <sup>60</sup>Cu-ATSM and <sup>64</sup>Cu-ATSM before beginning conventional treatment by chemoradiotherapy. All patients had locally advanced cervical cancer with primary lesions more than 2.0 cm in diameter. The women ranged in age from 33 to 79 y; their clinical FIGO (International Federation of Gynecology and Obstetrics) stages were IB1 in 1, IB2 in 1, IIB in 3, IIIA in 1, and IIIB in 4. The tumor

histology was squamous cell carcinoma in all patients. All patients gave written informed consent before participating in the study. All patients underwent clinically requested PET/CT with  $^{18}\text{F}$  FDG, as previously described (16). PET with  $^{60}\text{Cu}$ -ATSM and  $^{64}\text{Cu}$ -ATSM was performed with an ECAT HR+ scanner. Imaging with  $^{60}\text{Cu}$ -ATSM and  $^{64}\text{Cu}$ -ATSM was performed on separate days in a randomized order (4 patients underwent  $^{60}\text{Cu}$ -ATSM PET first and 6 patients underwent  $^{64}\text{Cu}$ -ATSM PET first). The time difference between the 2 scans averaged 5.8 d (range, 1–9 d). If  $^{60}\text{Cu}$ -ATSM was injected first,  $^{64}\text{Cu}$ -ATSM was injected at least 24 h (mean, 3.5 d; range, 1–7 d) after  $^{60}\text{Cu}$ -ATSM injection. If  $^{64}\text{Cu}$ -ATSM was injected first,  $^{60}\text{Cu}$ -ATSM was injected at least 6 d, that is, at least 11 half-lives of  $^{64}\text{Cu}$  (mean, 7.3 d; range, 6–9 d), after  $^{64}\text{Cu}$ -ATSM injection. For optimization of image quality, all 10 patients were to receive approximately 925 MBq (25 mCi) of  $^{64}\text{Cu}$ -ATSM and 740 MBq (20 mCi) of  $^{60}\text{Cu}$ -ATSM. These dosages of  $^{60}\text{Cu}$ -ATSM and  $^{64}\text{Cu}$ -ATSM were chosen to acquire the same number of decays in the 30- to 60-min-postinjection scan. A 925-MBq (25-mCi) dose of  $^{64}\text{Cu}$ -ATSM results in a 361 mGy dose to the liver and an effective dose of 33.3 mSv; the corresponding doses from a 740-MBq dose of  $^{60}\text{Cu}$ -ATSM are 47.4 mGy and 8.14 mSv, respectively (17). The imaging procedure and image processing were the same for both  $^{60}\text{Cu}$ -ATSM PET and  $^{64}\text{Cu}$ -ATSM PET except with regard to imaging mode and the treatment of the cascade  $\gamma$ -ray emission. The  $^{64}\text{Cu}$ -ATSM PET images were acquired in the 3D mode (with septa retracted) to maximize sensitivity. As for the phantom studies, all imaging with  $^{60}\text{Cu}$  was performed in the 2D mode, because the collimator septa minimize contamination by cascade coincidences. Where the injected activity of  $^{60}\text{Cu}$ -ATSM was less than the planned 740 MBq (20 mCi), the duration of image acquisition with  $^{64}\text{Cu}$ -ATSM was adjusted so that the images with both radionuclides had similar count statistics. Because the data from 30 to 60 min were acquired as six 5-min frames, the summed image was created from the approximate number of 5-min frames to achieve matching image statistics.

### Image Analysis

Clinical  $^{18}\text{F}$ -FDG PET/CT images were evaluated qualitatively with image interpretation criteria routinely used in scintigraphic imaging. For qualitative analysis, the  $^{60}\text{Cu}$ -ATSM PET and  $^{64}\text{Cu}$ -ATSM PET images were evaluated subjectively by an experienced nuclear medicine physician who was not aware of which copper-ATSM scan was being interpreted. Then, the images were evaluated in correlation with the CT and  $^{18}\text{F}$ -FDG PET/CT images. In addition, the overall tumor uptake of  $^{60}\text{Cu}$ -ATSM and  $^{64}\text{Cu}$ -ATSM

was assessed semiquantitatively by determining the tumor-to-muscle activity (T/M) ratio based on the 30- to 60-min summed images, as previously described (3–6,8). For the  $^{60}\text{Cu}$ -ATSM images, the patient data were processed by the cascade subtraction technique.

### Statistical Analysis

The tumor uptake of  $^{60}\text{Cu}$ -ATSM was correlated with that of  $^{64}\text{Cu}$ -ATSM to determine whether there was a relationship between the uptakes of these 2 radiotracers. *P* values less than 0.05 were considered statistically significant.

## RESULTS

### Phantom Data

The cylinder-to-uniform-area ratios are presented in Figure 1A for the peak values within the cylinder and in Figure 1B for the average values for  $^{64}\text{Cu}$  and  $^{60}\text{Cu}$  (with and without cascade subtraction). This phantom analysis indicates that similar cylinder-to-background ratios are observed for both radionuclides when cascade subtraction is used. The positron range of  $^{60}\text{Cu}$  is likely responsible for the reduced recovery coefficients observed for this nuclide.

### Patient Studies

There were no clinically significant changes in vital signs or laboratory test results after injection of  $^{60}\text{Cu}$ -ATSM and  $^{64}\text{Cu}$ -ATSM. No adverse events or clinically detectable pharmacologic effects related to either  $^{60}\text{Cu}$ -ATSM or  $^{64}\text{Cu}$ -ATSM were observed. The comparison study demonstrated increased  $^{60}\text{Cu}$ -ATSM and  $^{64}\text{Cu}$ -ATSM uptake in the tumors of all 10 patients (T/M ratios of  $5.9 \pm 1.6$  and  $7.3 \pm 1.9$ , respectively) (Table 1). The 10 patients received a mean of 903 MBq (24.3 mCi) (range, 821–952 MBq) of  $^{64}\text{Cu}$ -ATSM and a mean of 478 MBq (12.9 mCi) (range, 204–740 MBq) of  $^{60}\text{Cu}$ -ATSM (Table 1). A significant correlation was observed between the uptakes of  $^{60}\text{Cu}$ -ATSM and  $^{64}\text{Cu}$ -ATSM ( $r = 0.95$ ,  $P < 0.0001$ ) (Fig. 2). The image quality was comparable; although generally, the images with  $^{64}\text{Cu}$ -ATSM had a slightly better target-to-background ratio and tumors were delineated more clearly than on the  $^{60}\text{Cu}$ -ATSM images (Figs. 3A and 3B). Importantly, the pattern of uptake was similar on the images obtained with the tracers during 2 different imaging ses-

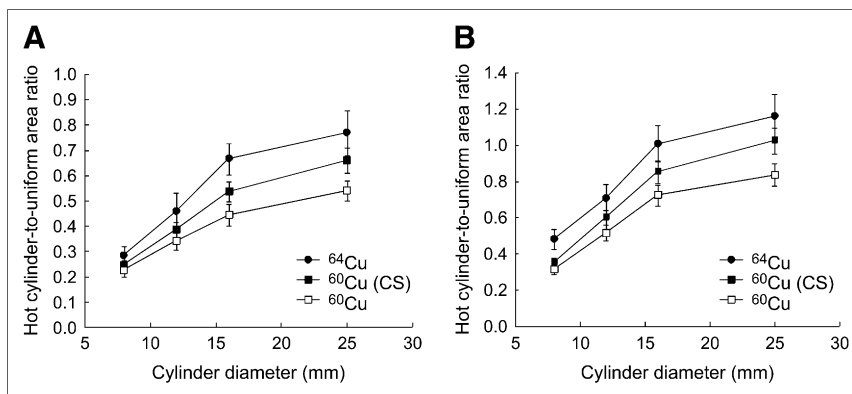


**FIGURE 1.** Activity ratios of hot cylinders to background, with cylinders of 8-, 12-, 16-, and 25-mm diameter for  $^{64}\text{Cu}$  and  $^{60}\text{Cu}$  (without and with cascade coincidence subtraction [CS]). Ratios of hot cylinder to uniform area in A are averages within cylinder and in B are peak values. Values were normalized to expected ratio of 9.87 to be equal to 1.

**TABLE 1**  
Summary of Patient Demographics and Imaging Comparison Results

Patient no.	Age (y)	Stage	First scan	Days between copper-ATSM scans	<sup>60</sup> Cu activity injected		<sup>64</sup> Cu activity injected		T/M ratio		
					MBq	mCi	MBq	mCi	<sup>60</sup> Cu	<sup>60</sup> Cu(CS)	<sup>64</sup> Cu
1	65	IIIA	<sup>60</sup> Cu	7	518	14.0	821	22.2	3.5	6.0	4.4
2	77	IIB	<sup>64</sup> Cu	9	352	9.5	918	24.8	5.7	6.3	7.2
3	33	IB1	<sup>64</sup> Cu	7	529	14.3	855	23.1	5.3	6.3	5.9
4	59	IIIB	<sup>64</sup> Cu	6	629	17.0	925	25.0	6.2	7.3	7.4
5	79	IIIB	<sup>60</sup> Cu	1	714	19.3	925	25.0	3.6	4.7	4.9
6	46	IIIB	<sup>64</sup> Cu	9	740	20.0	925	25.0	7.2	8.8	9.2
7	43	IIIB	<sup>60</sup> Cu	5	592	16.0	907	24.5	8.1	10.2	10.4
8	60	IIB	<sup>64</sup> Cu	7	204	5.5	925	25.0	7.9	9.8	8.4
9	45	IB2	<sup>64</sup> Cu	6	285	7.7	910	24.6	6.6	7.7	8.6
10	55	IIB	<sup>60</sup> Cu	1	222	6.0	895	24.2	5.0	5.9	7.1
Mean ± SD									5.9 ± 1.6	7.3 ± 1.8	7.3 ± 1.9

sions 1–9 d apart, indicating that the macroscopic distribution of hypoxia did not change greatly over this interval.

In addition, the patient data were quantitatively analyzed and T/M ratios were measured on the images obtained with <sup>64</sup>Cu-ATSM, <sup>60</sup>Cu-ATSM, and <sup>60</sup>Cu-ATSM processed with cascade subtraction (Fig. 2; Table 1). This analysis demonstrated that similar T/M ratios are obtained with both radionuclides and that application of the cascade subtraction correction improves the correlation between the <sup>64</sup>Cu-ATSM and the <sup>60</sup>Cu-ATSM measurements. The T/M ratio for <sup>60</sup>Cu-ATSM processed with cascade subtraction was

7.3 ± 1.8, closely similar to that reported for <sup>64</sup>Cu-ATSM. The slope of the regression line was 1.002 with the corrected <sup>60</sup>Cu-ATSM values, versus 1.238 without the cascade subtraction correction. The corresponding correlation coefficients were 0.88 and 0.95, respectively.

## DISCUSSION

Hypoxia is an important feature of solid tumors affecting tumor aggressiveness and response to therapy. Tumor hypoxia has been shown to be an adverse prognostic factor independent of standard prognostic factors such as tumor stage (18). In cervical cancer, direct assessment of tumor oxygenation by oxygen electrodes has demonstrated that patients with hypoxic tumors have worse disease-free survival than patients with nonhypoxic tumors (19). Although the oxygen electrode method is considered the gold standard for direct measurement of hypoxia, it is invasive, applicable only to accessible tumors, and technically difficult to perform, thus limiting its clinical use. Accordingly, noninvasive imaging methods such as PET have been studied as alternatives. We recently showed that the results of <sup>60</sup>Cu-ATSM PET predict prognosis in patients with locally advanced cervical cancer and rectal cancer (4,6). This method offers clinically relevant information that may have future applicability to directing hypoxia-targeted therapy.

Among the several radionuclides of copper, <sup>64</sup>Cu is the most commonly used for basic science investigations and clinical PET, and its production and use have now been reported in the United States, Europe, and Japan (20). With a half-life of 12.7 h, <sup>64</sup>Cu is ideally suited for PET studies that require a longer-lived nuclide: distribution of <sup>64</sup>Cu radiopharmaceuticals to facilities other than the production site is possible, and imaging can be conducted as long as 48 h after tracer administration. Moreover, because <sup>64</sup>Cu has a maximum positron energy of 0.66 MeV, similar to that of <sup>18</sup>F, the resulting PET images are of high quality and are the best obtainable with any of the positron-emitting radionuclides of copper. The 38.5% β<sup>-</sup> emission of <sup>64</sup>Cu opens the

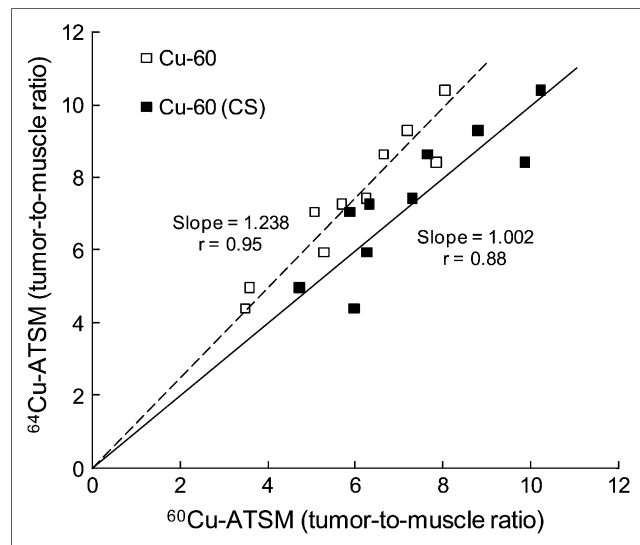


**FIGURE 2.** Correlation of <sup>60</sup>Cu-ATSM uptake (without and with cascade subtraction [CS]) and <sup>64</sup>Cu-ATSM uptake in 10 patients with cervical cancer. Results are expressed as T/M ratios. Good correlation between uptakes of these 2 radiotracers was found. This analysis was performed to demonstrate that similar T/M ratios can be obtained with both nuclides and that applying <sup>60</sup>Cu cascade coincidence correction improves comparability of measured T/M ratios. Linear regressions were determined by setting y-intercept to zero and slope derived from least-square minimization.

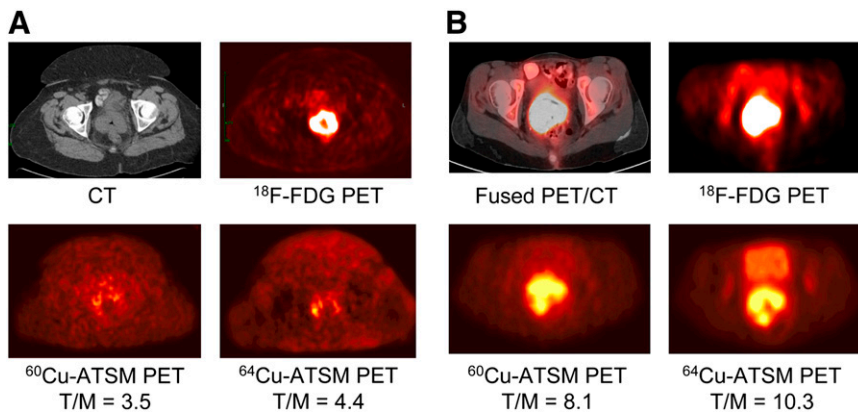


**FIGURE 3.** (A) Transaxial CT (top left) and  $^{18}\text{F}$ -FDG PET (top right) images of pelvis show intense  $^{18}\text{F}$ -FDG uptake within known cervical tumor at site of cervical mass seen on CT. Transaxial 30- to 60-min summed images of  $^{60}\text{Cu}$ -ATSM PET (bottom left) and  $^{64}\text{Cu}$ -ATSM PET (bottom right) of pelvis at same level demonstrate mildly increased uptake within known primary cervical tumor. There are similar patterns of  $^{60}\text{Cu}$ -ATSM and  $^{64}\text{Cu}$ -ATSM uptake within tumor. (B) Transaxial coregistered  $^{18}\text{F}$ -FDG PET/CT (top left) and  $^{18}\text{F}$ -FDG PET (top right) images of pelvis show intense  $^{18}\text{F}$ -FDG uptake within known cervical tumor at site of cervical mass seen on CT. Trans-

axial 30- to 60-min summed images of  $^{60}\text{Cu}$ -ATSM PET (bottom left) and  $^{64}\text{Cu}$ -ATSM PET (bottom right) of pelvis at same level demonstrate markedly increased uptake within known primary cervical tumor. There are similar patterns of  $^{60}\text{Cu}$ -ATSM and  $^{64}\text{Cu}$ -ATSM uptake within tumor.

possibility of therapeutic applications with this nuclide but adds a radiation burden to the patient when the nuclide is used for imaging purposes (7,21). This current work was undertaken to translate use of  $^{64}\text{Cu}$ -ATSM to humans, in order to allow for the production and supply of the radiopharmaceutical to multiple PET facilities. This process required a series of toxicology and pharmacology studies necessary to file an IND application with the FDA. These data demonstrated that the formulation has an appropriate margin of safety for clinical use. Thereafter, a small, cross-over bioequivalence study was performed to compare the quality of clinical PET images and the quantitative reproducibility of measured tumor uptake of copper-ATSM with  $^{60}\text{Cu}$  and  $^{64}\text{Cu}$  labeling.

After completion of the preclinical safety studies and submission of an IND application to the FDA, we studied patients with cervical cancer to assess whether the images obtained with  $^{64}\text{Cu}$ -ATSM are of similar quality to those obtained with  $^{60}\text{Cu}$ -ATSM.  $^{60}\text{Cu}$  decays by positron emission, with the concurrent emission of numerous  $\gamma$ -photons in cascade (most notably 826 keV, 21.7%; 1,333 keV, 88%; and 1,792 keV, 45.4%), originating from the  $\beta$ -decay to excited states in the  $^{60}\text{Ni}$  daughter nuclide. These additional  $\gamma$ -photons can downscatter into the acceptance energy window of the scanner and, as such, are not effectively suppressed. They will form fortuitous coincidences with incorrect positional information, thus increasing background activity and impairing image quality and quantitative accuracy. Those coincidences are typically not corrected adequately by the manufacturer-provided random or scatter corrections. Several techniques have been described for correction of cascade coincidences (15,22,23), but we used a convolution of the cascade  $\gamma$ -ray kernel, as previously reported (14). This technique was validated for  $^{86}\text{Y}$  and  $^{76}\text{Br}$  in a clinical tomograph operated in the 2D mode. In this technique, fully corrected projection data (corrected for normalization, attenuation, and scatter) are further corrected for cascade coincidence subtraction, and the images are then

reconstructed from those corrected data. After cascade subtraction, the hot-cylinder-to-background ratio for  $^{60}\text{Cu}$  became closer, but not equal, to that of  $^{64}\text{Cu}$ . This result is expected because of the longer positron range of  $^{60}\text{Cu}$ . Similar observations have been seen in other studies, where higher sphere-to-background ratios were observed after a uniform background subtraction was used (24,25). We chose here to use the deconvolution approach because it approximately accounts for the attenuation of the cascade  $\gamma$ -rays (14).

In our patient studies, we found that the image quality with  $^{64}\text{Cu}$ -ATSM was better than that with  $^{60}\text{Cu}$ -ATSM, but in most subjects fewer positron decays occurred during the 30- to 60-min  $^{60}\text{Cu}$ -ATSM scan than during the corresponding  $^{64}\text{Cu}$ -ATSM collection. In addition, the increased sensitivity ( $\sim$  by a factor of 2) of the 3D acquisition mode improved the statistics in the  $^{64}\text{Cu}$  images, resulting in improved image quality. The cascade subtraction technique does increase the image noise, especially in scans of low image statistics (because of short scan duration or low administered activity), but because of the relatively high statistics in our  $^{60}\text{Cu}$  patient images, this increase in noise was not a major problem. We found that the pattern and magnitude of tumor uptake of  $^{60}\text{Cu}$ -ATSM and  $^{64}\text{Cu}$ -ATSM on studies separated by 1–9 d were similar (Figs. 3A and 3B). Thus, tumor uptake of copper-ATSM appears to be reproducible regardless of the radionuclide used for imaging. It also appears that  $^{60}\text{Cu}$ -ATSM and  $^{64}\text{Cu}$ -ATSM measure a property of the tumor that is stable over time, likely related to chronic hypoxia as opposed to acute hypoxia (26). This finding is of importance given that the treatment of tumor hypoxia typically targets the chronic form of hypoxia.

The initial estimates of the injected activity for  $^{64}\text{Cu}$ -ATSM were based on previous imaging experience with  $^{60}\text{Cu}$  and on theoretic considerations regarding the relative half-life, positron decay branching ratio, and greater sensitivity in 3D mode relative to the 2D data acquisition mode of the PET scanner (17). The image quality obtained with

an injected dose of 925 MBq (25 mCi) of  $^{64}\text{Cu}$ -ATSM was excellent.

## CONCLUSION

The technology for production and widespread delivery of  $^{64}\text{Cu}$  is in place and commercialized. Several companies, including MDS Nordion (Canada), ACOM (Italy), Trace Life Sciences (United States), IBA Molecular (United States and Europe), and IsoTrace (United States) are supplying  $^{64}\text{Cu}$  for use in preparation of radiopharmaceuticals such as  $^{64}\text{Cu}$ -ATSM (20). Copper-ATSM has several well-known advantages over other radiopharmaceuticals used for PET of hypoxia (1,2), including a simpler method for synthesis, a faster clearance rate from normoxic tissue allowing a short time between injection and imaging, and a simpler method for quantification. All these qualities of  $^{64}\text{Cu}$ -ATSM make it an attractive tracer for clinical imaging of tumor hypoxia. This method can be used to identify patients for clinical trials of treatment strategies designed to overcome hypoxia.

## ACKNOWLEDGMENTS

We greatly appreciate the technical support by Linda Becker, Jennifer Frye, and Helen Kaemmerer. We also acknowledge Tom F. Voller, Lucie Tang, Todd A. Perkins, Dr. Rajendra Singh, Sally W. Schwarz, and the cyclotron staff at Washington University School of Medicine for their valuable assistance in the production of  $^{60}\text{Cu}$  and  $^{64}\text{Cu}$ . We also thank Dr. Brad Beattie (Memorial Sloan-Kettering) for sharing part of his program for the cascade subtraction. Toxicology and pharmacology studies were supported by the Development of Clinical Imaging Drugs & Enhancers (DCIDE) program of the Division of Cancer Treatment and Diagnosis (<http://imaging.cancer.gov/programsandresources/specializedinitiatives/dcide>) of the National Cancer Institute. This work was supported by NIH grant CA81525 and DOE grant DE-FG02-87ER60512.

## REFERENCES

1. Vavere AL, Lewis JS. Cu-ATSM: a radiopharmaceutical for the PET imaging of hypoxia. *Dalton Trans.* 2007;43:4893–4902.
2. Fujibayashi Y, Taniuchi H, Yonekura Y, Ohtani H, Konishi J, Yokoyama A. Copper-62-ATSM: a new hypoxia imaging agent with high membrane permeability and low redox potential. *J Nucl Med.* 1997;38:1155–1160.
3. Dehdashti F, Mintun MA, Lewis JS, et al. In vivo assessment of tumor hypoxia in lung cancer with  $^{60}\text{Cu}$ -ATSM. *Eur J Nucl Med Mol Imaging.* 2003;30:844–850.
4. Dehdashti F, Grigsby PW, Lewis JS, Laforest R, Siegel BA, Welch MJ. Assessing tumor hypoxia in cervical cancer by positron emission tomography with  $^{60}\text{Cu}$ -ATSM. *J Nucl Med.* 2008;49:201–205.
5. Dehdashti F, Grigsby PW, Mintun MA, Lewis JS, Siegel BA, Welch MJ. Assessing tumor hypoxia in cervical cancer by positron emission tomography with  $^{60}\text{Cu}$ -ATSM: relationship to therapeutic response—a preliminary report. *Int J Radiat Oncol Biol Phys.* 2003;55:1233–1238.
6. Dietz DW, Dehdashti FD, Grigsby PW, et al. Tumor hypoxia detected by positron emission tomography with  $^{60}\text{Cu}$ -ATSM as a predictor of response and survival in patients undergoing neoadjuvant chemoradiotherapy for rectal carcinoma: a pilot study. *Dis Colon Rectum.* In press.
7. Blower PJ, Lewis JS, Zweit J. Copper radionuclides and radiopharmaceuticals in nuclear medicine. *Nucl Med Biol.* 1996;23:957–980.
8. Chao C, Bosch WR, Mutic S, et al. A novel approach to overcome hypoxic tumor resistance: Cu-ATSM-guided intensity-modulated radiation therapy. *Int J Radiat Oncol Biol Phys.* 2001;49:1171–1182.
9. Haynes NG, Lacy JL, Nayak N, et al. Performance of a  $^{62}\text{Zn}/^{62}\text{Cu}$  generator in clinical trials of PET perfusion agent  $^{62}\text{Cu}$ -PTSM. *J Nucl Med.* 2000;41:309–314.
10. McCarthy DW, Bass LA, Cutler PD, et al. High purity production and potential applications of copper-60 and copper-61. *Nucl Med Biol.* 1999;26:351–358.
11. McCarthy DW, Shefer RE, Klinkowstein RE, et al. Efficient production of high specific activity  $^{64}\text{Cu}$  using a biomedical cyclotron. *Nucl Med Biol.* 1997;24:35–43.
12. PET Phantom Instructions for Evaluation of PET Image Quality. American College of Radiology Web site. Available at: [https://www.acr.org/accreditation/nuclear/qc\\_forms/FeaturedCategories/qc\\_forms/PET\\_Phantom\\_Instructions.aspx](https://www.acr.org/accreditation/nuclear/qc_forms/FeaturedCategories/qc_forms/PET_Phantom_Instructions.aspx). Accessed April 21, 2008.
13. Adam LE, Zaers J, Ostertag H, Trojan H, Bellemann ME, Brix G. Performance evaluation of the whole-body PET scanner ECAT EXAT HR + following the IEC standard. *IEEE Trans Nucl Sci.* 1997;44:1172–1179.
14. Beattie BJ, Pentlow KS. A correction for cascade coincidences in 3D utilizing the delayed coincidence sinogram [abstract]. *J Nucl Med.* 2004;45(suppl):411P.
15. Beattie BJ, Finn RD, Rowland DJ, Pentlow KS. Quantitative imaging of bromine-76 and yttrium-86 with PET: a method for the removal of spurious activity introduced by cascade gamma rays. *Med Phys.* 2003;30:2410–2423.
16. Wright JD, Dehdashti F, Herzog TJ, et al. Preoperative nodal staging of early stage cervical carcinoma by FDG-PET. *Cancer.* 2005;104:2484–2491.
17. Laforest R, Dehdashti F, Lewis JS, Schwarz SW. Dosimetry of  $^{60}\text{Cu}/^{62}\text{Cu}$ -ATSM: a hypoxia imaging agent for PET. *Eur J Nucl Med Mol Imaging.* 2005;32:764–770.
18. Vaupel P, Mayer A. Hypoxia in cancer: significance and impact on clinical outcome. *Cancer Metastasis Rev.* 2007;26:225–239.
19. Höckel M, Schlenger K, Aral B, Mitze M, Schäffer U, Vaupel P. Association between tumor hypoxia and malignant progression in advanced cancer of the uterine cervix. *Cancer Res.* 1996;56:4509–4515.
20. Lewis JS, Welch MJ, Tang L. Workshop of the production, application and clinical translation of “non-standard” PET nuclides: a meeting report. *Q J Nucl Med Mol Imaging.* 2008;52:101–106.
21. Lewis J, Buettner TL, Connett JM, Fujibayashi Y, Welch MJ. Cu-64-diacetyl-bis( $\text{N}^4$ -methylthiosemicarbazone): an agent for radiotherapy. *Proc Natl Acad Sci.* 2001;98:1206–1211.
22. Biggot HM, Laforest R, Liu X, Ruangma A, Wuest F, Welch MJ. Advances in the production, processing and microPET image quality of technetium-94m. *Nucl Med Biol.* 2006;33:923–933.
23. Buchholz HG, Herzog H, Forster GJ, et al. PET imaging with yttrium-86: comparison of phantom measurements acquired with different PET scanners before and after applying background subtraction. *Eur J Nucl Med Mol Imaging.* 2003;30:716–720.
24. Herzog H, Quaim SM, Tellman L, Spellerberg S, Kruecker D, Coenen HH. Assessment of the short-lived non-pure positron-emitting nuclide  $^{120}\text{I}$  for PET imaging. *Eur J Nucl Med Mol Imaging.* 2006;33:1249–1257.
25. Lubberink M, Schneider H, Bergstrom M, Lundqvist H. Quantitative imaging and correction for cascade gamma radiation of  $^{76}\text{Br}$  with 3D and 3D PET. *Phys Med Biol.* 2002;47:3519–3534.
26. Brown JM. The hypoxic cell: a target for selective cancer therapy—Eighteenth Bruce F. Cain Memorial Award Lecture. *Cancer Res.* 1999;59:5863–5870.